



Formation of a barrier island breach and its contributions to lagoonal circulation

Alireza Gharagozlu ^{a,*}, J. Casey Dietrich ^a, T. Chris Massey ^b, Dylan L. Anderson ^a, Jessica F. Gorski ^a, Margery F. Overton ^a

^a Dep't of Civil, Construction, and Environmental Engineering, NC State University, Campus Box 7908, 915 Partners Way, Raleigh, NC, 27695, United States of America

^b Coastal and Hydraulics Laboratory, U.S. Army Engineer Research and Development Center, 3909 Halls Ferry Road, Vicksburg, MS, 39180, United States of America

ARTICLE INFO

Keywords:

Hatteras Island
Hurricane Isabel
XBeach
ADCIRC+SWAN

ABSTRACT

Barrier islands are a primary coastal defense and often experience erosion during storms. When they fail due to storm-induced breaching, there can be significant changes to the small- and large-scale hydrodynamics and morphodynamics of the region. In this study, we explore the formation of a breach on Hatteras Island, North Carolina, during Isabel (2003) and the subsequent flooding into Pamlico Sound. Two-way coupling of high-fidelity, high-resolution numerical models for coastal erosion and flooding enables a better understanding of the formation of the breach, as well as scenarios of the breach's effects on the circulation in the region. The breach connecting the ocean to the sound formed during the day of landfall. It is shown that, during the storm, overwash and inundation from the ocean led to deterioration of the beach and dunes, and then after the storm, the creation of channels through the island was sensitive to elevated water levels in the lagoon. Then flooding scenarios are considered in which the ground surface of the hydrodynamic model was (a) static, updated with the (b) pre- and post-storm observations, and updated dynamically with (c) erosion model predictions and (d) erosion model predictions with elevated lagoon-side water levels. The model results show that the breach has region-scale effects on flooding that extend 10 to 13 km into the lagoon, increasing the local water levels by as much as 1.5 m. These results have implications for similar island-lagoon systems threatened by storms.

1. Introduction

Coastal storms can cause significant morphological changes to barrier islands, as demonstrated by the numerous breaches in the past 10 years due to Irene (2011) in North Carolina (Clinch et al., 2012), Sandy (2012) in the mid-Atlantic coast (Sopkin et al., 2014), Isaac (2012) in Louisiana (Sherwood et al., 2014), Matthew (2016) in the southeast-Atlantic coast (Birchler et al., 2019), and Michael (2018) in northwest Florida (FEMA, 2020). When these breaches are initiated, they can allow flooding into lagoons that were otherwise protected, e.g. into the bays on Long Island (Canizares and Irish, 2008), often with negative effects on the lagoonal ecosystem, e.g. the rapid changes in water quality in Barnegat Bay due to island breaching during Sandy (Miselis et al., 2016; Smalley and Irish, 2017). These events are likely to occur more often due to rising sea levels (Passeri et al., 2015) and as storms become stronger due to climate change (Kossin et al., 2020; Emanuel, 2020), increasing the likelihood of beach erosion, breaching, and coastal flooding. Predictions of the morphodynamic

response of the beach and its impact on the regional circulation are crucial for flood risk assessment.

Researchers understand the causes for discrete erosion events. The morphodynamic response can be categorized from the swash regime, where the waves and water levels impact only the beach, to the inundation regime, where overland flow can cause dune erosion and breaching (Sallenger, 2000). Barrier islands can be inundated and eroded from both the ocean- (van Ormondt et al., 2020) and lagoon-sides (Safak et al., 2016), and flow can concentrate within low areas to scour a channel (Pierce, 1970). Although barrier islands can be large, breaches often occur in specific locations (Fritz et al., 2007; Sallenger et al., 2007; Fearnley et al., 2009). Barrier island erosion and breaching can be linked to island width (Morton, 2002), persistent rip channels (Thornton et al., 2007), offshore wave conditions (Gracia et al., 2013), and geologic formations like relict river channels (Riggs et al., 1995).

* Corresponding author.

E-mail address: aghara@ncsu.edu (A. Gharagozlu).

Predictive morphodynamic models are applied typically for studies on small domains, due both to their computational cost and the need to resolve the dune-scale coastal features (e.g. dune shape, small inlets) and physical processes (Elsayed and Oumeraci, 2017). The eXtreme Beach (XBeach) model (Roelvink et al., 2009) has evolved significantly during the last decade to better predict storm effects on coastal regions. Early studies used bulk parameters within the models to control erosion, such as limiting the Shields parameter of erosion and overwash in Santa Rosa Island during Ivan (2004) (McCall et al., 2010). However, later studies have represented the effects of land covers (e.g. sand, vegetation, pavement) as multiple sediment layers (Kurum and Overton, 2013) or spatially varying bottom friction, like for the erosion and overwash in Dauphin Island (Passeri et al., 2018). Physics-based improvements were implemented in XBeach to account for dilatancy and bed slope (de Vet, 2014) and for temporally-varying bed roughness (van der Lught et al., 2019), thus allowing for predictions of the general behavior of the barrier breaching. In a study of erosion along the mid-Atlantic coast due to Sandy (2012) and Matthew (2016), the model was able to predict some of the breach locations, but not all of them, and the predicted channel depths were shallower than observed after the storm (van der Lught et al., 2019). These results are encouraging for risk assessment; even a limited prediction of barrier breaching can be useful to locate vulnerabilities in the overall system. However, more research is needed to improve understanding of how breaches form and evolve during storms.

Storm surge in a shallow lagoonal system can contribute to the flooding of nearby communities. These effects can be predicted with region-wide models for wind waves, tides, and circulation (Dietrich et al., 2013), but these models often include a static ground surface. For Ike (2008) in Texas, it has been shown that the early easterly winds pushed water into the communities on the west side of Galveston Bay, which was later flooded by storm surge through the Bolivar Roads inlet and over Galveston Island and the Bolivar Peninsula (Sebastian et al., 2014). In North Carolina (NC), wave-induced set-up contributes to inundation along the ocean-side of the Outer Banks (Sheng et al., 2010) and throughout the Pamlico and Albemarle Sounds (Mulligan et al., 2015). For the few studies in which barrier erosion was included, the simulations used a static ground surface with the post-storm topography and bathymetry (Canizares and Irish, 2008). These studies have shown the removal of the Chandeleur Islands in Louisiana could increase surge by 0.5 m near New Orleans (Wamsley et al., 2009) and wave heights by nearly 500 percent, while restored islands could delay the peak surge by 1 to 2 h (Grzegorzewski et al., 2009), although the effect is spatially variable (Grzegorzewski et al., 2011). Similarly, erosion on Bolivar Peninsula could increase the surge volume in Galveston Bay by 50 to 60 percent (Rego and Li, 2010). While these studies have shown the importance of the barrier island system, they did not include the timing of erosion and breaches and their effects on flooding and surge on the back-barrier.

Recent studies with a tight coupling of hydro- and morphodynamics have shown that adjustment of the ground surface to represent beach and dune erosion can improve accuracy of flooding predictions (Velasquez et al., 2015), including for storm surge along the Outer Banks of North Carolina (Gharagozlu et al., 2020). Herein, we extend these studies to also consider storm-induced breaching and its contribution to lagoonal circulation. We hypothesize that: (1) the breaches were formed due to the combined effects of ocean-side erosion of the beach and dunes during the storm and lagoon-side elevated water levels and scour after the storm, and (2) the evolving breach can affect the timing and extent of flow into the lagoon. We test these hypotheses via simulations of a breach on Hatteras Island, NC, during Isabel (2003), which is well-described with pre- and post-storm observations of the island topography and a post-storm survey of the breach bathymetry. First, a high-resolution, morphodynamic simulation of the so-called ‘Isabel Inlet’ is validated and then used to understand the evolution of the breaches. The model predicts the initiation of the breach during the day of the storm’s

landfall and its approximate location, even with minimal information about variations in subsurface and sediment properties. However, there are differences between the channels’ exact locations and depths as predicted by the erosion model and observed in the post-storm surveys. Then a larger-domain circulation model is applied for simulations in which the ground surface is (a) static, updated linearly between the (b) pre- and post-storm observations, and updated dynamically with the (c) full breach evolution from the morphodynamic model and (d) full breach evolution with elevated sound-side water levels. The results show that the breach can affect circulation more than 10 km into the lagoon.

2. Methods

2.1. Storm and study area

Isabel was the most powerful storm during the 2003 Atlantic hurricane season (Beven and Cobb, 2003). It formed as a tropical depression and then a tropical storm on 6 September, and it increased in intensity over the next five days. Isabel became a Category-5 hurricane by 18:00 UTC 11 September with maximum sustained winds estimated at 74 m/s. It continued to move northwestward over the next several days, weakening to a Category-2 hurricane on 16 September. Isabel maintained this intensity through its landfall near Drum Inlet in the Outer Banks at 17:00 UTC 18 September (Beven and Cobb, 2003) (Fig. 1). Its winds, waves, and storm surge affected most of coastal North Carolina. Isabel generated waves with maximum significant heights of about 8.1 m at the US Army Corps of Engineers (USACE) Field Research Facility in Duck, NC. At the ocean-side of Cape Hatteras, the National Oceanic and Atmospheric Administration (NOAA) gauge recorded a total water level of 2.05 m before failing during the storm (Hovis et al., 2004). The waves and surge caused damages to infrastructure (Rogers and Tezak, 2004) and made significant changes to the landscape (Sallenger et al., 2004).

The largest individual erosion event occurred near the western end of Hatteras Island, about 60 km east of Isabel’s landfall location. The island topography was surveyed with Light Detection and Ranging (LiDAR) (Bonisteel et al., 2009) on 16 Sep, about two days before landfall, and again on 21 Sep, about three days after landfall. The LiDAR vertical and horizontal accuracies were within 0.3 m and 1 m, respectively (Fredericks et al., 2017). Before the storm, the island was narrowest with a width of about 150 m at this section (Fig. 2, top), and the dune crest elevation was lower than other points along the island (Wamsley and Hathaway, 2004). During the storm, the island was breached, and the village of Hatteras became inaccessible due to the 520-m inlet that formed to connect the ocean and the sound. The newly formed inlet geometry was surveyed on 13–16 Oct, about four weeks after landfall (Fig. 2, middle), when two ‘breach islands’ separated the opening into three channels. The western channel was filled with debris and had a width of about 105 m with a maximum depth of 2 to 3 m, whereas the middle breach channel was 70 m wide and relatively shallower than the other channels with a maximum depth of 1.5 m. The middle channel only flooded at higher tide elevations because a peat terrace restricted the flow on the ocean side of this channel. The main channel on the east side was approximately 100 m wide on the sound side and 105 m wide on the ocean side. The unrestricted flow through this channel created scour depths down to 6 m (Wamsley and Hathaway, 2004) and consequently allowed more flow during ebb tide. The so-called ‘Isabel Inlet’ was closed by the U.S. Army Corps of Engineers (USACE) on 1 Nov (Wurtkowsky, 2004).

These surveys provide valuable information about the island topography immediately before the storm and the channel geometries a few weeks after the storm. However, they are imperfect, because it is possible that the breach channels evolved and deepened in the weeks following the storm. It is noted that there were no observations of the ground surface on the island during the storm, and the only nearby

gauge was a NOAA water-level station on the ocean side that failed before the storm peak. Recent studies have observed overland flow (Engelstad et al., 2017) and groundwater gradients (Sherwood et al., 2014) during island inundation events, but data (especially ground surface data) are not available during a catastrophic breaching event. Thus, it is common to use pre- and post-storm surveys with multiple-week spacings to evaluate the start and end point of breaching (Safak et al., 2016; Sherwood et al., 2014; van der Lught et al., 2019).

For this study, we assume that the majority of the erosion occurred during the storm's day of landfall, when the waves and surge were largest. The survey data were interpolated into high-resolution DEMs using the regularized spline tension method (Mitasova et al., 2005) (Fig. 2). The DEMs have 1-m resolution and represent detailed topographic features. For the pre-storm DEM, we use the LiDAR survey from 16 Sep (about two days before landfall) to represent the sub-aerial ground surface on Hatteras Island. For the post-storm DEM, we use the LiDAR survey from 21 Sep (about three days after landfall) to represent the sub-aerial ground surface, and we use the USACE survey from 13–16 Oct (about four weeks after landfall) to represent the bathymetry in the breaches. These surveys are merged into a single post-storm DEM.

2.2. Models

2.2.1. ADCIRC+SWAN

The ADvanced CIRCulation (ADCIRC) (Luettich et al., 1992; Westerink et al., 2008) and Simulating WAves Nearshore (SWAN) (Booij et al., 1999) models are used to predict the region-wide effects of Isabel on nearshore waves and circulation. The models are widely-used for storm surge and coastal flooding (Hope et al., 2013; Cyriac et al., 2018; Suh et al., 2015) and have been validated for applications along the U.S. Gulf (Dietrich et al., 2018) and Atlantic (Thomas et al., 2019) coasts. ADCIRC uses the continuous-Galerkin finite element method to solve modified forms of the shallow water equations on unstructured meshes. SWAN solves the wave action density equation for the evolution of wave energy, and was extended to use unstructured meshes (Zijlema, 2010). ADCIRC+SWAN are dynamically coupled to use the same mesh and allow information to pass through local memory without the need for interpolation between models (Dietrich et al., 2011b). The coupled models can provide predictions of water levels, depth-averaged currents, and wave parameters (significant height, peak period, etc.) throughout a large domain, but with focused resolution in the coastal region of interest.

We used an edited version of the high-resolution NC9 mesh (v9.98) (Blanton and Luettich, 2008), with increased resolution in the NC coastal region (Fig. 1). The resolution of the mesh varies from 100 km in the Atlantic Ocean to 50 m in the nearshore of NC. The mesh extends inland to the 15-m topographic contour to allow for storm surge and flooding prediction. Ground elevations at the mesh vertices were interpolated from several high-resolution DEMs to resolve bathymetric and topographic features such as inlets, dunes and rivers (Blanton and Luettich, 2008; Blanton et al., 2008). The typical mesh resolution on Hatteras Island was about 50 m, and thus the beach and dune system was represented with only 1–2 elements in the cross-shore direction. In this study, to improve the representation near the breach, the maximum resolution was increased to about 20 m on the Outer Banks near the Hatteras Inlet. This resolution was selected to represent the shape of the breach in the model and also based on mesh sensitivity studies (Gharagozlu et al., 2020). Then the ground surface was re-interpolated from the pre-storm DEM.

The SWAN+ADCIRC simulations are for 23 days, with a 15-day tides-only simulation from 00:00 UTC Aug 28 to 00:00 UTC Sep 12, and then an 8-day storm simulation until 00:00 UTC Sep 20. ADCIRC uses a time step of 1 sec (due to the constraints of its wet/dry algorithm and the Courant–Friedrichs–Lewy condition), while SWAN uses a time step (and coupling interval) of 1200 sec (due to its implicit solver). Tides are specified with 8 harmonic constituents (M_2 , S_2 , N_2 , K_2 , K_1 , O_1 , P_1 ,

and Q_1). From land-use/land-cover data, spatially varying inputs are included for bottom stress, which is computed from Manning's n values, and surface stress, which is reduced both partially due to overland roughness and fully due to blocking from forest canopies (Westerink et al., 2008). Average horizontal eddy viscosities are specified in two classes of $2 \text{ m}^2/\text{s}$ and $10 \text{ m}^2/\text{s}$, while the primitive weighting in the modified continuity equation is specified in three classes of 0.005, 0.02, and 0.03. Advective terms are enabled. SWAN settings are similar to previous studies (Thomas et al., 2019; Dietrich et al., 2018). For the transfer of momentum to the wave and circulation models, the wind drag coefficient has an upper limit of 0.002; this is balanced in ADCIRC with no lower limit on the bottom friction coefficient.

Atmospheric pressure and wind velocities from OceanWeather Inc. (Cox et al., 1995) are used as surface forcings for waves and circulation. The wind fields consist of surface pressures and wind velocities between 00:00 UTC Sep 12 and 00:00 UTC Sep 20 at 15-minute intervals and on a nested set of regular grids with the coverage over 60° to 85° W longitude and 15° to 48° N latitude. Surface pressures and wind velocities fields are interpolated in time and space onto the unstructured mesh used by ADCIRC+SWAN. Fields developed with this technique have been used in ADCIRC hindcasts of Katrina (Dietrich et al., 2010), Gustav (Dietrich et al., 2011a), Ike (Hope et al., 2013), and other storms.

2.2.2. XBeach

The eXtreme Beach (XBeach) model is used to predict the evolution of the breach on Hatteras Island during the storm. In ‘surfbeat’ mode, XBeach accounts for the waves motion by solving the time-varying, short-wave action balance equation on wave-group scale to generate the radiation stresses. The model solves the depth-averaged nonlinear shallow water equations for mean flow and includes dissipation (Roelvink, 1993) and roller models (Svendsen, 1984). XBeach also includes the effects of infragravity waves by resolving the short wave variation and the long waves associated with them. Sediment transport is modeled with a depth-averaged advection–diffusion equation, and bed elevations are updated according to the Exner equation. The model is capable of simulating the morphodynamic behavior of coastal dune systems under different storm impact regimes with excellent skill, as shown in other studies (Passeri et al., 2018; van der Lught et al., 2019).

The model is calibrated using several parameters for bed friction, sediment transport, hydrodynamics, and wetting/drying and avalanching processes. These parameters differ from the default XBeach settings, but the selected values are consistent with other recent studies. To keep the dunes and the shape of the channels stable, the critical avalanching slope for the wet nodes is increased to $wetslp = 0.6$. We use $f_{mor} = 10$ (McCall et al., 2010) to speed up the morphological evolution relative to the hydrodynamic time scale. Instead of the Shields parameter S_{max} , a uniform bed friction coefficient of $C = 30$ (Nederhoff, 2014) is used in the model. Additionally, the effect of wave asymmetry and skewness is included by increasing $\gamma_{ua} = 0.18$. XBeach default settings tend to overestimate the erosion, so a non-physics-based approach was introduced (McCall et al., 2010) to hinder the erosion by limiting the Shields parameter. This method improves the results when the beach is in the overwash or collision regime. However, a physics-based approach to implement the land cover effects is suggested in recent studies (Passeri et al., 2018; Schambach et al., 2018), which used spatially-varying bed friction coefficient derived from land cover DEMs, where each type of coverage is assigned an equivalent Manning's n coefficient. A formulation was implemented in XBeach to account for vegetation impact by temporally changing the bed friction relative to the thickness of erosion and sedimentation (van der Lught et al., 2019). In this study, a uniform bed friction value was used to simplify the model and keep it applicable to other regions. Thus, the main morphodynamic behavior of the barrier system is determined by the topography and bathymetry of the region and the hydrodynamic forcing.

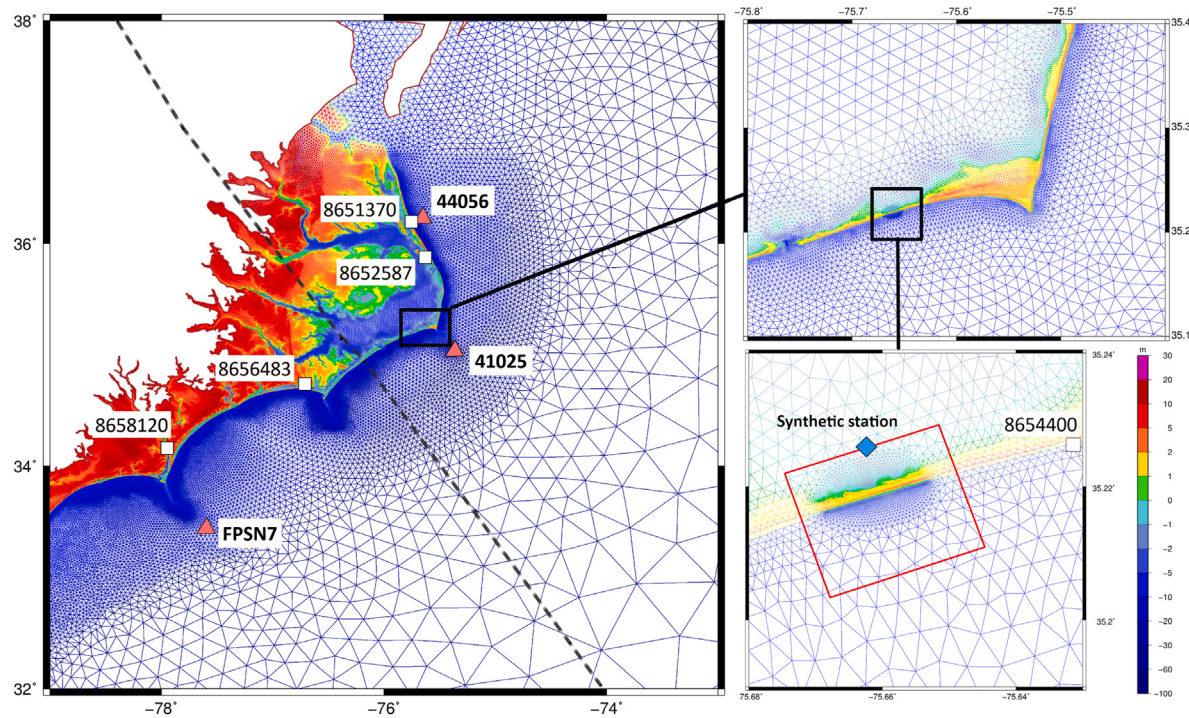


Fig. 1. ADCIRC mesh coverage on North Carolina coast. Isabel's track is shown with a dashed line. The study area in Hatteras Island and the boundary of the XBeach domain (red box) are shown. The red triangles and white squares show the locations of NDBC buoys and NOAA gauges, respectively. Description of these stations and model validation of wave heights and water levels are provided in Gharagozou et al. (2020). In the bottom right figure, the location of the NOAA gauge that failed before Isabel's landfall is shown. Additionally, a synthetic station (blue diamond) is considered to show the wind velocity, direction, and water level time series on the sound side (Fig. 3), which will be used as the back-shore boundary conditions in XBeach.

XBeach is applied on a domain with a total alongshore length of about 2.2 km (Fig. 1). Using the DEM created from the pre-storm survey, a high-resolution mesh was generated to represent the bathymetry and topography of the barrier island with the focus on the breached inlet. The model resolves this ground surface by using a structured mesh with 600 cells along-shore and 490 cells across-shore. To allow for development of waves at the boundary, the mesh extends 1.5 km offshore and 0.8 km on the lagoon side. The domain is extended beyond the depth of closure so the hydrodynamics can adjust to the nearshore conditions before they impact the sub-aerial portion of the domain. Mesh resolution varies locally in the cross-shore direction with minimum cell spacing of 2 m on the island and maximum of 20 m at the offshore boundary. The alongshore spacing also varies between 2 m and 10 m, with the minimum spacing located on the breach location. The model runs for three days of the storm starting at 00:00 UTC Sep 17. This XBeach start is five days later than the ADCIRC+SWAN start, and thus the waves and circulation will adjust to the atmospheric forcing before they are applied as boundary conditions to the morphodynamics.

2.2.3. Two-way coupling of XBeach and ADCIRC+SWAN

A one-way coupling is common, with predictions of the larger-domain waves and flooding to be used as boundary conditions for the smaller-scale erosion (Passeri et al., 2018; Schambach et al., 2018). However, a two-way coupling is considered herein.

To XBeach, boundary conditions for water levels and waves were taken from ADCIRC+SWAN predictions (described above). Time series of water levels were applied at both the offshore and the lagoon boundaries. Waves can be applied at only one boundary, therefore the time series of SWAN wave parameters (significant height, peak period, and mean direction) were only applied at the offshore boundary. This information is used by XBeach to generate a JONSWAP spectrum with $\gamma = 3.3$ and directional spreading of 20, which is consistent with similar studies on the U.S. Atlantic (Schambach et al., 2018) and Gulf coasts (Passeri et al., 2018). The XBeach model interpolates the input

boundary conditions spatially and temporally to generate values along its boundaries.

To ADCIRC, a dynamic approach for updating the topography was developed and implemented in version 53 of the ADCIRC source code; this approach allows the model to modulate the elevation of the nodes during simulation and incorporate the variation of the bed level due to erosion and deposition. Repeatedly during the simulation, the model reads data about the time-varying bathymetry, updates the ground surface elevations at the mesh vertices, and then continues with its computations. This method is not strictly mass-conserving (and this is a direction for future research) and relies on other sources to predict the ground surface variations spatially and temporally. However, it does allow ADCIRC to represent the effects of the morphodynamics while maintaining model stability. Additional information about the parameters and setup of this dynamic approach is provided in Appendix. In this study, we use the dynamic bathymetry update to include the erosion and breaching of the barrier island in ADCIRC.

3. Results

3.1. Storm effects near Hatteras Island

The storm's effects on waves and water levels are described at several locations (Fig. 1). Observations are available at the NDBC buoys ranging from deep water to nearshore and at NOAA gauges along the NC coast. The maximum significant wave heights were 8.1 m at a gauge near Duck, NC, and the peak water level was 2.05 m at a gauge on the ocean-side at Cape Hatteras. A validation of ADCIRC+SWAN predictions of waves and water levels is included in Gharagozou et al. (2020). Here, it is noted that the gauge at Cape Hatteras failed before the peak of the storm, and there were no other gauges near the breach location to observe how waves and water levels varied on the ocean- and sound-sides. A synthetic station is selected on the sound side of the breach, where the boundary of the XBeach domain is located (Fig. 1,

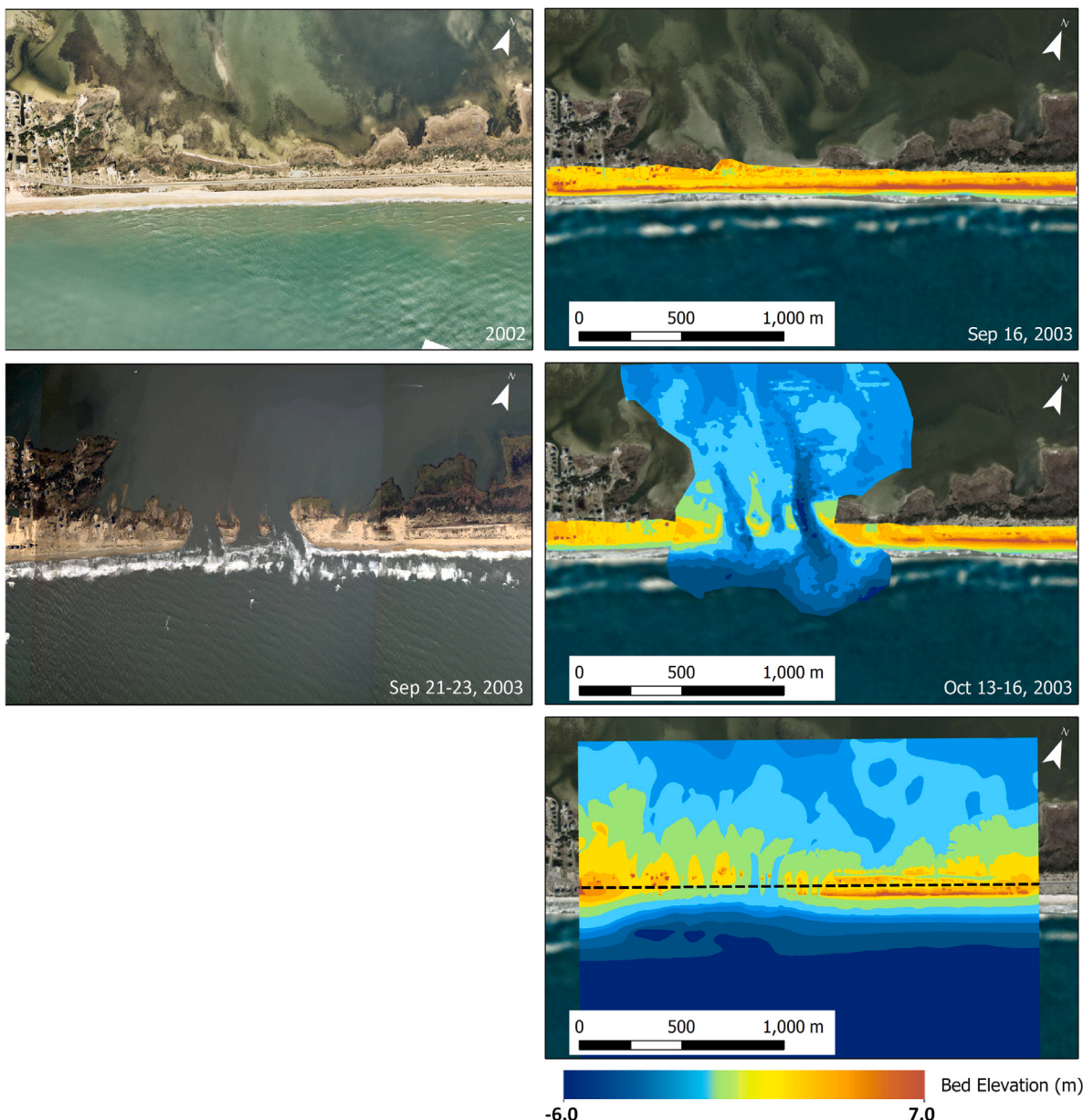


Fig. 2. Isabel Inlet as described by pre- and post-storm (left) satellite images and (right) surveys and model predictions. The surveys were used to derive DEMs to represent (top-right) pre-storm and (middle-right) post-storm conditions. Three eroded channels were observed in the post-storm survey, with the deepest channel on the east side. The three breaches had a combined width of 500 m. These DEMs were used to initialize and validate the (bottom) XBeach-predicted final bathymetry and topography, with the 2 distinct channels in the middle and extensive dune erosion on the west side. The dashed line shows the transect of the alongshore profile, where the flow rate through the island was calculated in Fig. 5.

bottom right) and the predicted wind speeds, wind directions, and water levels at this location are shown in Fig. 3. The wind speed was less than 15 m/s until 00:00 Sep 18. As the storm approached the region, the wind speeds increased to a maximum of about 39 m/s on 15:00 UTC Sep 18. The wind directions changed as the eye of the storm passed the barrier island. The wind direction changed abruptly from 250° at 8:00 Sep 18 to 90° at 18:00 Sep 18, with directions measured counter-clockwise from east.

The ADCIRC predictions are critical at this location, because they will be used as boundary conditions to the XBeach simulations of the island breach, which we will show was sensitive to waves and surge from both the ocean- and sound-sides. (For Isabel, the rainfall and runoff were not significant contributors to the water levels at Hatteras Island during the storm (Beven and Cobb, 2003).) Sound-side seiching and surge have been observed during recent storms, e.g. the rapid increase of water levels near Oregon Inlet during Arthur

(2014) (Cyriac et al., 2018), or the multiple breaches of the Core Banks during Dorian (2019) (Sherwood et al., 2020). In those storms, both the observations and model predictions showed elevated water levels, up to 1 m above mean sea level, in the sound for 12 to 24 h after the storm landfall. However, in our ADCIRC simulation for Isabel, although the water levels are predicted to drawdown before landfall and then return to normal conditions, they are not predicted to rise and sustain at an elevated level after landfall. There was no sound-side gauge with observations to validate these water levels, but they may be an underprediction, similar to the ADCIRC underprediction by more than 0.5 m of the peak surge at Oregon Inlet during Arthur (2014) (Cyriac et al., 2018). This underprediction may be caused by the relatively coarse temporal resolution of the atmospheric forcing, which slows the change in wind direction that is the primary cause of seiching and surge, and/or the bottom friction parameterization in Pamlico Sound, which may not account for muddy bottoms and lower

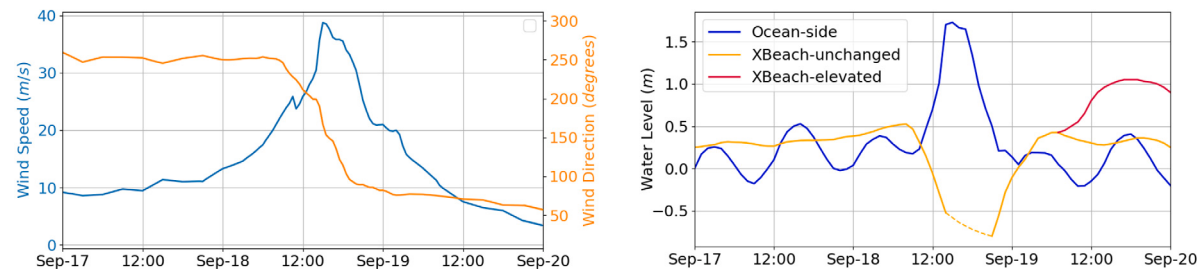


Fig. 3. Storm effects at a synthetic station on the lagoon side of the breach (with location in Fig. 1): (left) OWI wind speeds (m/s) and directions (degrees counter-clockwise from east); and (right) ADCIRC-predicted water levels (m) at the ocean (blue) and at the sound side when unchanged (orange) and elevated (red). (For interpretation of the references to color in this figure legend, the reader is referred to the web version of this article.)

friction that would allow seiching and surge to propagate to the Outer Banks. Thus, to test our first hypothesis in the following analyses, we apply boundary forcing to XBeach simulations with two scenarios: with ADCIRC water levels as predicted on the sound side, and with ADCIRC water levels but elevated artificially to 1 m above mean sea level for the last 12 h of the XBeach simulation. These two scenarios of sound-side water levels are shown in Fig. 3. It is noted that the elevated water levels are applied only as boundary conditions to XBeach; the water levels are not elevated artificially in any ADCIRC simulations to follow.

3.2. Erosion and breaching at Isabel Inlet

We next explore the breaching of the Isabel Inlet by using XBeach to predict its timing and evolution at high resolution. We consider both qualitative (shape, location, and timing of the breach) and quantitative (volumetric sediment change and flowrate) characteristics of the breach. The focus is to understand how the storm waves and surge impacted the beach and dune system, how the breach was formed, and what were the channel depths immediately after the storm (before they could be deepened further by tidal currents).

3.2.1. Timeline of island response

The XBeach simulation covers 3 days of Isabel, starting at 00:00 UTC Sep 17 until 00:00 UTC Sep 20. At Hatteras Island, the peak of the storm occurred during the second day of the simulation, which is also when the channels developed through the island. At the start of the simulation (Fig. 4a), the storm was 41 h and 860 km from landfall. The ocean-side water level was less than 0.5 m (relative to NAVD88), and thus only the foreshore and the beach were eroded. However, the waves and water levels increased as the storm approached the coast. Later at 07:00 UTC Sep 18 (Fig. 4b), the storm was 10 h and 310 km from landfall. On the ocean side, the total water level due to waves, surge, and tide was larger than 1.0 m (NAVD88), and thus it extended to and started to erode the dune toe. By 14:00 UTC Sep 18 (Fig. 4c), ocean water flowed through the dunes at a low point in the dune crest for beach access, and then spread alongshore to flood the road and other parts of the back-dune.

During the next 2 h, severe dune erosion occurred, specifically in the middle and west parts of the domain. This prediction is in agreement with post-storm data that show the dunes on the west side were removed completely. The eroded sand was deposited in front of the dunes on the beach area. This collision process weakened the dune system by lowering the crest and reducing the dune thickness until 16:00 UTC Sep 18, when it switched to the overwash and inundation regimes (Fig. 4d). When the storm was about to make landfall, the dunes had already been flattened. Strong flow and inundation through the island moved a considerable volume of sand to the back bay area. The topography of the island conveyed the flow through a specific section, which later led to the formation of channels. The water level then began to recede on the ocean side as the surge on the sound side increased. At 06:00 UTC Sep 19, about 13 h after landfall, the water

level on the sound exceeded the ocean side which forced a gradual back flow to the ocean (Fig. 4e).

During the last 18 h, the water flowed from the sound through the small channels, causing them to deepen. However, the channel depths were highly sensitive to the size of this water-level gradient across the island. For the scenario with the unchanged ADCIRC water levels as sound-side boundary conditions (Fig. 4f-i), the flow conditions were not sufficient to scour the channels to have depths below sea level through the island. Instead, although the beach and dune have been eroded away, there is still a land connection. However, for the scenario with the elevated water levels as sound-side boundary conditions during the last 12 h of the simulation (Fig. 4f-ii), the channels were scoured to depths below sea level, and sediment was moved to the ocean side.

These findings provide a better understanding of the island response to the storm, especially the temporal evolution of the dune erosion and channel formation. The dunes protected the barrier island from flooding during the early part of the storm; however, sustained surge and waves weakened the system and eventually removed the dunes. The island topography conveyed the water flow through low-lying areas or possibly through smaller channels that had been scarped behind the dunes historically. In the narrow section of the island, the back flow from the lagoon side to the ocean formed and deepened the channels, but the amount of scour was sensitive to the water-level gradient across the island.

3.2.2. Rates and quantities of erosion and discharge

To better understand the erosion and breaching process, we calculated the erosion rate and total volumetric change of sand on the sub-aerial part of the island. This information agrees with the storm phases and additionally can inform the coupling with the flooding model. A total volume of about 160 000 m³ was removed during the XBeach simulation (Fig. 5 top). Initially, the erosion rate was very small and most of the sediment transport occurred on the beach. At 06:00 UTC Sep 18, the total water level reached the dunes. The erosion and deposition increased, and dunes eroded rapidly. However, because the sand was deposited in front of the dunes, the erosion rate during this time was about 2500 m³/h. The cumulative erosion volume until 14:00 UTC Sep 18 was 40 000 m³. At the peak of the storm, the most significant erosion of the dunes occurred, which resulted in 90 000 m³ volume of sand loss at a rate of 13 000 m³/h. This large erosion occurred mostly on the middle and west side of the domain and comprised about 55 percent of the total sand loss over 7 to 8 h. At 00:00 UTC Sep 19, the erosion slowed down, and the water level decreased on the ocean side. For the scenario with elevated water levels on the sound side, a returning flow from the sound to the ocean eroded and deepened the channels. This scour caused an additional 10 000 m³ of erosion, compared to the scenario with unchanged water levels.

We also computed the discharge along 2 km of the island where the breaching occurred (red lines in Fig. 5 bottom). For about half of the simulation time, the dunes protected the barrier island from inundation. However, erosion of the dunes during this time lowered the crest and, at 14:00 UTC Sep 18, the overwash and flow through

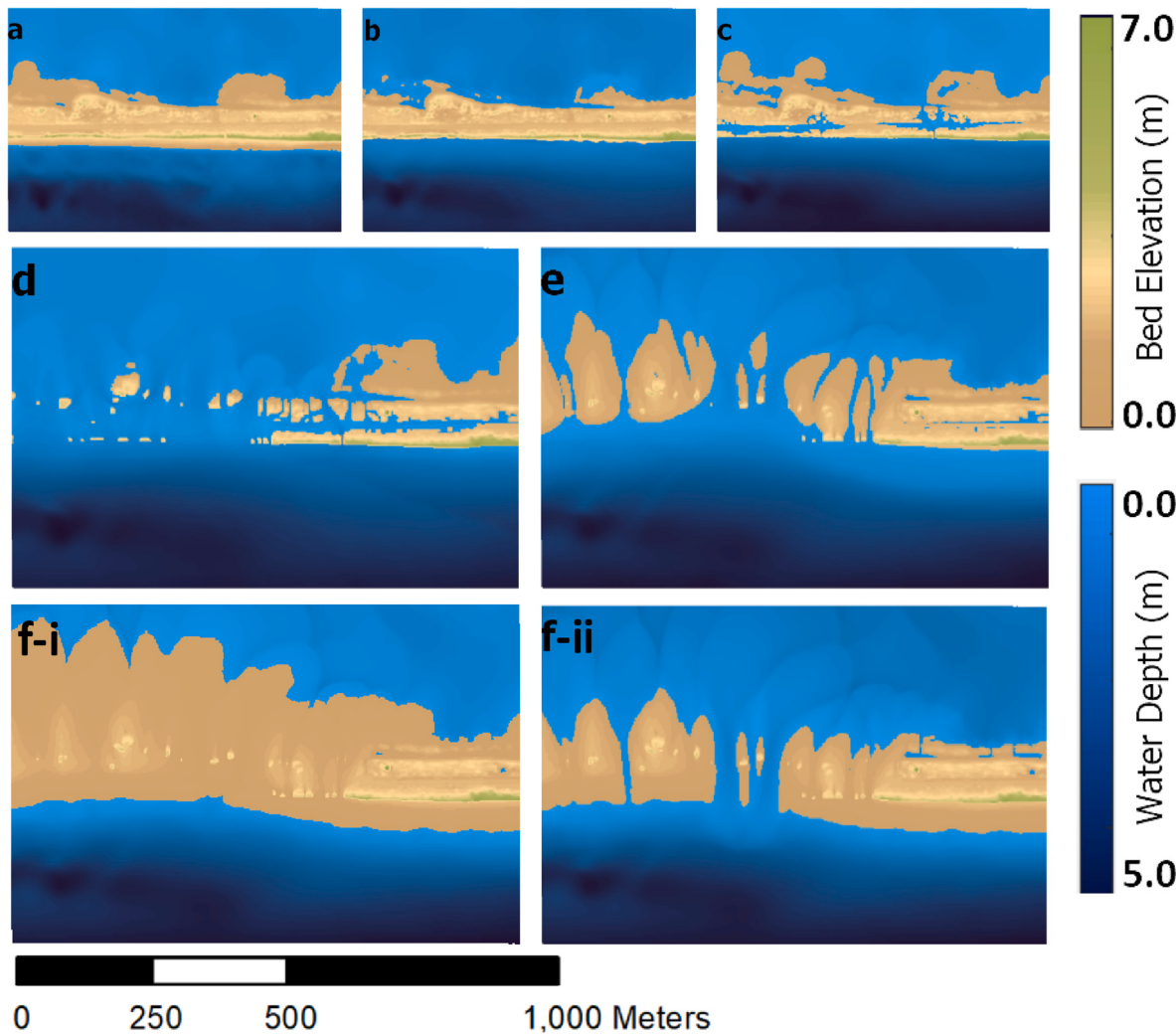


Fig. 4. XBeach-predicted evolution of the Isabel Inlet: (a) the initial state at 00:00 UTC Sep 17; (b) the collision regime at 7:00 UTC Sep 18; (c) at 14:00 UTC Sep 18 when the overwash and flooding through beach access occurred; (d) at 16:00 UTC Sep 18, when the overwash and inundation on the west side of the domain occurred; (e) at 06:00 UTC Sep 19, the water level on the sound side exceeded the ocean side; (f-i) the final condition at 00:00 UTC Sep 20 using ADCIRC-predicted sound-side water levels with shallow channels; and (f-ii) the final condition at 00:00 UTC Sep 20 using elevated sound-side water levels with two deeper channels in the middle of the domain.

beach access increased the discharge. At 16:00 UTC Sep 18 with the dunes removed entirely, maximum discharge of $1300 \text{ m}^3/\text{s}$ was reached, corresponding to extensive inundation on the west and middle of the domain. Then the discharge decreased as the water level increased on the sound side. The direction of the current flowed between the ocean and the sound until 12:00 UTC Sep 19. After this time, there is almost no flow through the island for the XBeach (unchanged) scenario. However, for the XBeach (elevated) scenario, the water level gradient caused scour across the island and deepened the channels. Note the difference in discharge due to the higher sound-side water levels during the last 12 h in the XBeach (elevated) results; the maximum discharge was about $190 \text{ m}^3/\text{s}$, compared to no discharge for the unchanged sound-side water levels as predicted by ADCIRC.

3.3. Breaching effects on larger-scale circulation

We next consider the storm's effects on the larger-scale circulation and flooding, via the coupling with ADCIRC+SWAN. Although similar models can predict the morphodynamics of large sand sheets or waves and nearshore evolution, morphodynamics of island breaches are dependent on local gradients in sediment transport, the scale of which is not feasible in larger-domain models like ADCIRC. Therefore the ground surface elevations at its mesh vertices are typically fixed during

the simulation. In our first simulation with two-way coupling, we use (a) a static bathymetry, in which the pre-storm DEM is interpolated onto the mesh. Then in following simulations with two-way coupling, we allow the bathymetry to evolve. The time-varying bathymetry information is extracted from (b) a hypothetical linear transition from pre-storm to post-storm DEMs of the bathymetry and topography, (c) an XBeach simulation of island erosion with the unchanged ADCIRC boundary conditions, and (d) an XBeach simulation of breaching with the elevated sound-side water levels. It is noted that, in these ADCIRC simulations, the water levels are not increased artificially; instead, they will respond to the varying scenarios of ground surface evolution.

3.3.1. Static scenario

In the static scenario, the ground surface elevation was fixed during the simulation, and thus the erosion during the storm was not included. Figs. 6a show time snaps of the static mode before the storm peak, during the maximum surge, after the landfall, and the final condition. At 17:00 UTC Sep 18 when the maximum surge reached the coast, the water level on the ocean side was about 2.0 m (Fig. 6a-iii). On the sound side, however, the wind pushed the water back and created a dry region behind the barrier island. At 00:00 UTC Sep 19, this region was flooded again as the water returned (Fig. 6a-iv). The final results show that a fully-intact dune system would protect the barrier island from extensive flooding (Fig. 6a-v).

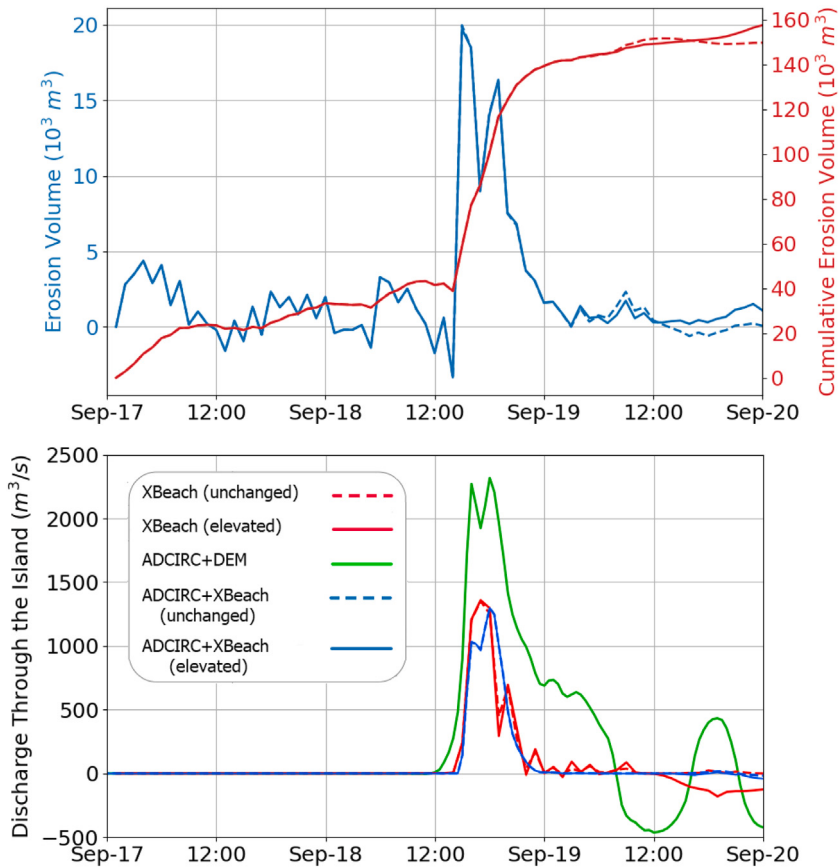


Fig. 5. Erosion and discharge through the breach (with location in Fig. 2: (top) erosion volume (m^3) and cumulative total sand loss (m^3) on the sub-aerial part of the barrier island during the storm, and (bottom) flow discharge (m^3/s) through the island during storm calculated from XBeach (red) as well as ADCIRC with surveys (green) and XBeach (blue). (For interpretation of the references to color in this figure legend, the reader is referred to the web version of this article.)

3.3.2. Dynamic scenario with pre- and post-storm DEMs

The ground surface was updated dynamically in the ADCIRC simulation by using the pre- and post-storm DEMs. The initial elevation was obtained from the pre-storm DEM, corresponding to the island topography about two days before landfall. Then the elevation of each vertex was changed to reach the post-storm DEM, which has a combination of the topographic and bathymetric surveys collected after the storm. Because the exact timing of the breach cannot be known, we assume the major morphodynamic changes occurred during the storm's day of landfall. Thus, in the ADCIRC simulation, these ground-surface changes are applied linearly, starting at 00:00 UTC Sep 18 and continuing over 24 h.

In this scenario, the ground surface elevation was reduced during the simulation, and the channels developed as the storm approached the coast. This process allowed water to flood the barrier and cross the island onto the sound. At 06:00 UTC Sep 18, the elevation of the deeper channel was low enough to allow water to intrude the island from the sound side (Fig. 6b-i). At 14:00 UTC Sep 18, three hours before landfall, the dunes were lowered and inundation occurred on the island (Fig. 6b-ii). At 17:00 UTC Sep 18, the maximum surge flooded the island and the channels were deep enough to facilitate flow through the island (Fig. 6b-iii). Contrary to the static scenario where the sound side became dry temporarily, in this scenario, the flow from the ocean to the sound kept the region flooded with a maximum water level of 1.2 m. After landfall, the wind pushed the water back toward the ocean. In the static scenario, the water piled on the sound side behind the barrier island, however, in this scenario, the channels conveyed the water back to the ocean and equalized the water level on both sides (Fig. 6b-v).

For this scenario, the flow discharge through the barrier island was computed based on the current velocity and the depth of the

water. Initially, the dunes prevented flooding into the island, however, when the elevation of the dunes reduced to below the total water level, flooding started at 12:00 UTC Sep 18. If the ground surface had eroded in this manner during the peak of the storm, then the flowrate would have increased rapidly reaching 2300 m^3/s (Fig. 5 bottom). The flowrate reduced to 750 m^3/s over the next 6 h with current restricted to the shallowly formed channels. At 07:00 UTC Sep 19, the storm pushed water from the sound back to the ocean, and the flowrate reached 500 m^3/s at 12:00 UTC Sep 19. During the last 12 h of the simulation, the channels were formed fully and allowed for water pass. The oscillations in the discharge graph correspond to the tide and ebb flows through these channels. The total volume of water exchanged between ocean and sound during the storm was about 58 million cubic meters.

Additionally, the maximum of differences in water level and current velocities between this mode and the static mode was calculated. Maximum difference is about 1.8 m in this scenario compared to the static scenario (Fig. 7a-i). The differences in water level are limited to the sound near the breach extending to the northeast side. However, the differences near the northern part of Hatteras Island are caused by small delays in the phase of wetting and drying, and thus the main impact of the breach is observed roughly within 10 km of the opening and on the sound side. The velocity differences show a similar pattern with maximum differences near the breach of about 3 m/s (7a-ii).

To examine the current through the inlet and the larger-scale effects of the breach, we represented the flow with 20 Lagrangian particles. Their movement is based on the depth-averaged velocities as reported by ADCIRC (Dietrich et al., 2012). The particles were released on the sound side at 06:00 UTC Sep 18, a few hours before the breaching started. Fig. 7a-iii shows the tracks of these particles over time. Initially

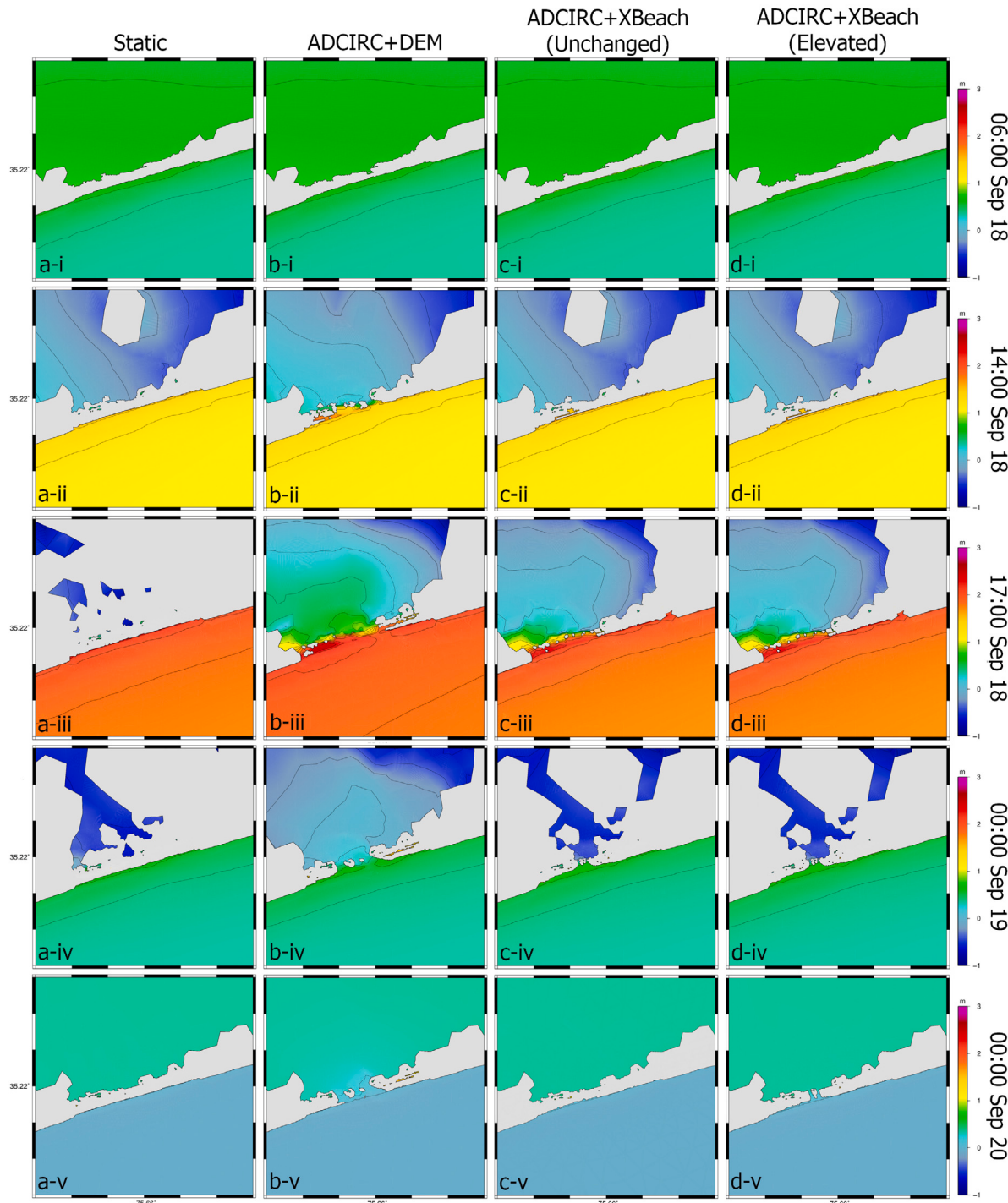


Fig. 6. Water elevation during the storm in (a) static mode, (b) ADCIRC+DEMs, (c) ADCIRC+XBeach (unchanged), and (d) ADCIRC+XBeach (elevated). The water levels are shown at different time snaps during the storm.

the particles are pushed into the sound in the northwest direction. Then, at 18:00 UTC Sep 18, they turn east and eventually follow a path northward. During the 40 h after the breach is opened, these particles move northward 35 km (and far beyond the extents of the XBeach domain), thus demonstrating the breach's contribution to the circulation in the larger Pamlico Sound.

3.3.3. Dynamic scenarios with XBeach

The XBeach simulations, which ideally include more realistic details of flood water timings and magnitudes, were also used to dynamically update the ground surface in ADCIRC. In these case, the ground surface

elevation data are extracted hourly during the 3-day XBeach simulations, and then inverse-distance weighting (IDW) interpolation is used to upscale the XBeach-predicted bed levels onto the ADCIRC mesh.

Similar to the previous scenario, the results show that the barrier island was inundated and water passed through the breached channels. Initially, the dune system on the barrier island prevented the flooding until 14:00 UTC Sep 18 when the total water elevation on the ocean side exceeded the eroded dune crest, and overwash occurred (Fig. 6c-ii and d-ii). This was similar to the XBeach prediction at 14:00 UTC Sep 18 (Fig. 4c). The flooding through the island reached its maximum at

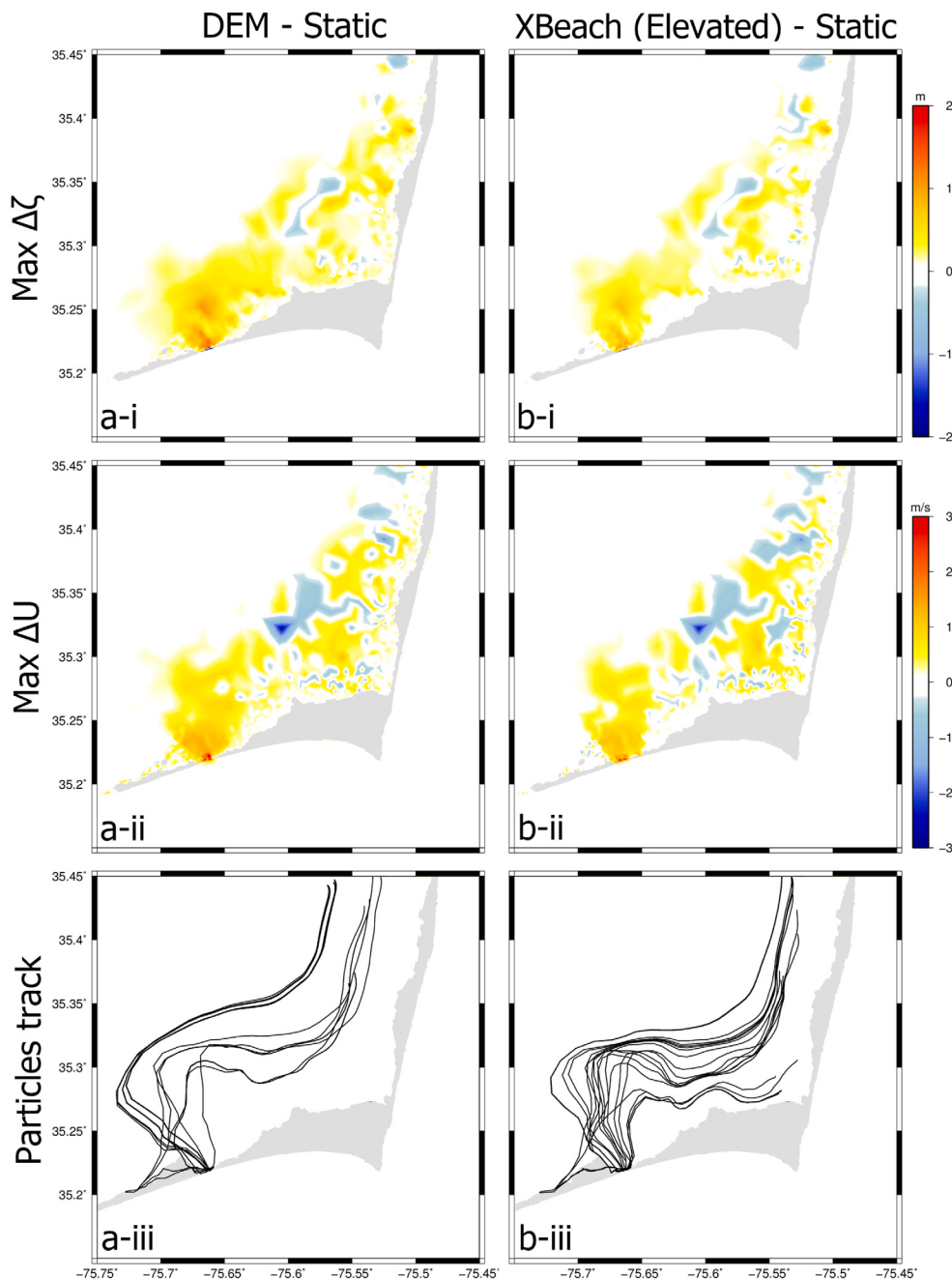


Fig. 7. Maximum difference of water level (top) and velocity (middle) between (a) ADCIRC+DEMs and static mode, and (b) ADCIRC+XBeach (elevated) and static mode. The particle tracks (bottom) are shown for ADCIRC+DEMs and ADCIRC+XBeach (elevated) simulations. Note the differences and particle tracks for the ADCIRC+XBeach (unchanged) results were nearly identical to the ADCIRC+XBeach (elevated) results, and thus they are not shown.

17:00 UTC Sep 18 when the storm made landfall (Fig. 6c-iii and d-iii). The flooding extent was smaller compared to the ADCIRC+DEM results, and the water level elevation on the sound side was lower. This is because the channels predicted by XBeach were not as wide and deep as in the post-storm DEM. The dune system on the island was eroded but the channels were not fully formed, thus the volume of water crossing the barrier was limited. At 00:00 UTC Sep 19, the water on the sound was pushed back, but the flow through the small channels filled the region. However, some areas were still dry (Fig. 6c-iv and d-iv). At 06:00 UTC Sep 19, the water level on the sound side increased and exceeded the ocean side water level, which forced a flow from the sound back to the ocean. In the case of XBeach (unchanged), the barrier island elevation is higher than water levels on both sides (Fig. 6c-v). However, in the case of XBeach (elevated), the deeper channels connect

the ocean and the sound until the end of the simulation at 00:00 UTC Sep 20 (Fig. 6d-v).

The discharge computed for this scenario shows that the flooding started at 14:00 UTC Sep 18, or about 2 h later than the previous scenario. The discharge through the island was 1250 m³/s during the peak of the storm (Fig. 5 bottom). Compared to the ADCIRC+DEM scenario, this flowrate was much smaller (about 50% less). The total volume of water exchanged between the ocean and sound in this case was about 19 million cubic meters, which was 33% of the volume calculated for the previous scenario, however, it was similar to the XBeach prediction for discharge through the barrier island.

The maximum of differences in water level and velocities between the ADCIRC+XBeach (elevated) scenario and the static scenario are shown in Fig. 7b. The maximum water level difference was 1.5 m

near the breach. Similar to the ADCIRC+DEM scenario, the differences are observable near the beach and further on the north-east along the sound-side of the barrier island (Fig. 7b-i). The plume of water extends about 10 km in the sound, but it is slightly smaller than in the previous scenario. The maximum depth-averaged velocity difference is about 2.5 m/s compared to the static scenario (Fig. 7b-ii).

The track of particles released on the sound is qualitatively similar to the previous scenario (Fig. 7b-iii). However, the particles start to move into the sound half an hour later, due to a later opening of the breach in the XBeach predictions. Also, the particles do not extend as far to the west in the sound, and instead they track closer to the sound-side of Hatteras Island as they move northward. Thus, with a lower flow volume through the breach, the effects did not extend as far into Pamlico Sound.

4. Discussion

These results have several implications for our understanding of the formation of the Isabel Inlet and its effects on the larger circulation in Pamlico Sound, as well as our ability to predict breaches due to other storms.

XBeach predicted the Isabel Inlet breach with reasonable accuracy, similar to other studies (Elsayed and Oumeraci, 2017; Nederhoff, 2014). The model represents the collision, overwash, and inundation regimes at appropriate times as the storm approached and made landfall, and the erosion of the dunes on the west side is comparable to the observations (Fig. 2). Most importantly, the predicted breach is at the correct approximate location of the Isabel Inlet. These predictions were achieved with minimal model tuning — the sediment properties are uniform through the model domain, there is no use of a non-erodible layer, and the other model settings were derived from recent studies (as referenced in Section 2.2.2). These results are encouraging for the use of XBeach in regions where the subsurface properties are uncertain, and for coupling with larger-domain flood models for real-time predictions.

However, the predicted number, shape, and depth of the channels are not fully accurate, at least in comparison with the post-storm survey. In the XBeach prediction, two channels are breached, and they are located at 840 m and 930 m from the west boundary (Fig. 8), which match the location of the western and middle channels in the post-storm survey. A third channel should have been breached and all channels should be deeper and wider. In the XBeach prediction, the two channels have similar depths and widths of about 0.45 m and 40 to 50 m, respectively. In the post-storm survey four weeks after the storm, the three channels have widths of 105 m, 70 m, and 105 m, with the maximum depth of 6 m on the eastern channel.

These inaccuracies are likely caused by a combination of factors. First, the prediction of island breaching, especially the sub-aqueous transport to create channels, may be beyond the capabilities of XBeach. Several recent studies have focused on island breaching (de Vet, 2014; Nederhoff, 2014; Elsayed et al., 2018; van der Lugt et al., 2019) with similar results — the locations of the breaches are generally correct, but XBeach fails to erode channels to their full depths. Second, the subsurface geology can affect and control the erosion. Reports of this breach have mentioned the appearance of a peat layer (Wamsley and Hathaway, 2004; Wurtkowski, 2004), which would focus the erosion in the channels. The configuration of the peat layer is unknown, and thus it is not represented in our model. Third, the channel depths may be exaggerated in the post-storm survey, which was conducted a few weeks after landfall. A newly formed inlet can have a highly dynamic morphology, and the tidal current through the channels and ocean waves can change the shape and depth of the channel. It may not be reasonable to compare the XBeach-predicted channels immediately after the storm with the real channels as surveyed a few weeks later. Taken together, these factors are an indication that, although our simulation is a good qualitative depiction, it should be considered as one possible scenario of the island's response to the storm.

It is appropriate to consider several scenarios of how the breach may have affected the larger-scale circulation. The dynamic ADCIRC simulations show that including the morphodynamics can change the hydrodynamics and the flooding pattern significantly because the newly formed channels were deep enough to allow a considerable flow discharge through the island. In the scenario with the ground surface from the DEMs, we assumed a linear change in ground surface elevation can represent the morphodynamics, but this may not be an accurate match to the response of the barrier island. For example, in this scenario at 06:00 UTC Sep 18, flooding was initiated on the sound side (Fig. 6b-i), when the immediate impacts of surge and waves were on the ocean side. Because of the linear transition of the ground surface in time, it was reduced to below mean sea level too early and before the storm affected the sound side. In contrast, in the scenario with the ground surface from XBeach (elevated), the flooding was initiated from the ocean side at the appropriate time (Fig. 6c,d-ii). These scenarios show the channels conveyed water to maintain the elevated water levels on the sound side during the peak of the storm, and then also conveyed water to equalize the water levels between the ocean and sound after the storm.

The true flowrate through the breach was likely somewhere between these two scenarios. In the scenario with the ground surface from the post-storm survey, the channels were probably too deep, and thus the discharge of 2300 m³/s was too high. In the scenario with XBeach, the channels were underpredicted in width and depth, and thus the discharge of 1250 m³/s was probably too low. These scenarios are useful in that they provide a reasonable range for the true flowrate, and they are motivation for improved observation of subsurface properties to constrain the morphodynamic model predictions.

The maximum differences in water level show that erosion of the dunes on the barrier island as predicted by XBeach can impact the hydrodynamics on the sound at larger scales. However, compared to the case with a linear variation of the ground surface between the pre- and post-storm DEMs, the maximum differences are smaller in the XBeach cases both for water level and current velocity. Although the channel depths and widths in the DEM-based case were much larger than in the XBeach-based cases, the extent of water level, velocity differences, and particle tracks are similar in all cases. The particles tracks inside the lagoon are impacted by the wind force and the tidal current inside the lagoon, however, the breaching allows the water to push the particles from the sound-side shore further into the lagoon.

These results show that region-scale circulation can be affected by a breach. Consequently, higher water levels on the sound can result in local flooding in nearby communities, such as the town of Hatteras. These larger scale impacts can only be studied with a coupled model that resolves the temporal and spatial evolution of the breach and the subsequent flow through the barrier island. The plume jet through the breach extends to several kilometers into the lagoon and creates strong currents that push the particles into the lagoon. The extent of the region affected by the breach, both in terms of water level and current velocity, is several orders larger than the width of the breach, which again demonstrates the importance of small-scale morphodynamic changes on larger-scale hydrodynamics.

5. Conclusions

In this study for Isabel (2003), XBeach and ADCIRC+SWAN were coupled to predict the small-scale morphodynamics of breaching on Hatteras Island and its effects on lagoonal circulation in Pamlico Sound. We used a time-varying bathymetry module to dynamically update the ground surface elevation in ADCIRC+SWAN and represent the evolution of the breach. The dynamic mode was implemented both by using the DEMs and XBeach model predictions, and the results were compared to the static mode, in which the bathymetry is fixed. The flooding of the island during the storm was explored, and the flowrate for each case was calculated. The major findings of this study are:

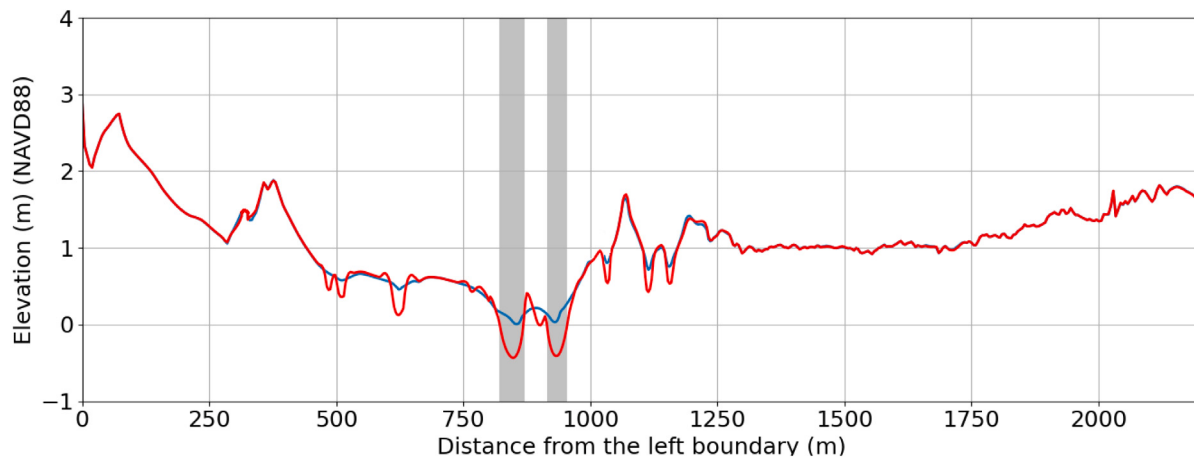


Fig. 8. Alongshore profile of the XBeach-predicted final ground surface, for (blue) XBeach (unchanged) and (red) XBeach (elevated) (red). With the elevated water levels on the sound side, the formed channels are deeper by about 0.5 m. The location of this profile is shown with the dashed line in Fig. 2. The locations of the breached channels are highlighted. These channels are located at $x = 850$ m and $x = 920$ m from the left (west) boundary of the XBeach domain. (For interpretation of the references to color in this figure legend, the reader is referred to the web version of this article.)

1. *With a simple model setup and minimum tuning of the parameters, XBeach could predict the initiation and location of the breach.* This simplicity will allow the model to be applicable to other locations. Further improvement of the results may require additional parameterization (e.g. spatially varying friction, multiple sediment layers, vegetation impact, etc.). Although the predicted depth and number of the breached channels did not match the conditions from several weeks after the storm, the information about the temporal evolution of the breach was useful for predicting the interaction of the breach with large-scale hydrodynamics near the barrier island.
2. *Flow from the sound to the ocean has an important role in deepening the breached channels.* Although there are no observations of water levels in the sound near the breach, the model predictions show that water level gradient from the sound to the ocean scarped the channels and increased the depth of the breach. These results support the behavior seen in Dorian (2019) (Sherwood et al., 2020), in which returning flow from the sound to the ocean may have caused breaching in the same barrier system.
3. *Breaching of the barrier island has significant large-scale impacts on the hydrodynamics.* When XBeach predictions of the temporal evolution of the erosion are included in an ADCIRC+SWAN simulation with a dynamic ground surface, a more realistic representation of the breach is captured by the model. The water level increased by 1 m near the breach, and the ocean waters extended to 13 km into the sound. These scenarios provide a reasonable range for the flow pattern through the breach, and they improve predictions of hazards from the sound side at nearby residential communities.

These results emphasize the need to consider coastal erosion in the prediction of storm surge and coastal flooding during storms, especially for real-time forecasting. Future studies will extend to other storms and coastal regions, further explore the applicability of a simple XBeach model setup (spatially uniform sediment properties, parameters from published studies) to predictions of coastal erosion in a range of settings, and automate the two-way coupling of a dynamic ground surface in ADCIRC+SWAN. These advancements will continue to improve our understanding of how barrier-island breaching can significantly change the water levels and circulation in lagoonal systems.

CRediT authorship contribution statement

Alireza Gharagozlu: Methodology, Investigation, Writing – original draft. **J. Casey Dietrich:** Conceptualization, Funding acquisition,

Writing – review & editing. **T. Chris Massey:** Software. **Dylan L. Anderson:** Writing – review & editing. **Jessica F. Gorski:** Investigation. **Margery F. Overton:** Supervision.

Declaration of competing interest

The authors declare that they have no known competing financial interests or personal relationships that could have appeared to influence the work reported in this paper.

Acknowledgments

This project is funded, in part, by the U.S. Coastal Research Program (USCRP) as administered by the U.S. Army Corps of Engineers (USACE), Department of Defense, under Grant Award Number W912HZ18C0026. The content of the information provided in this publication does not necessarily reflect the position or the policy of the government, and no official endorsement should be inferred. The authors acknowledge the USACE and USCRP's support of their effort to strengthen coastal academic programs and address coastal community needs in the United States.

Appendix

ADCIRC has a (relatively undocumented) module for time-varying bathymetry, which allows for changes to the ground surface during the simulation, thus representing the morphodynamics or any variation in ground surface elevation. These changes are implemented by altering the ground surface elevation at specified mesh vertices and over specified durations. Then an offset equal to the ground surface change ($\partial h / \partial t$) is added to the water level change ($\partial \eta / \partial t$), to maintain the total water depth at that location. For example, if the ground surface is lowered by 1 cm at a vertex, then the water surface is also lowered by 1 cm. Then the mass and momentum conservation equations are solved for the new water surface elevations and velocities, respectively, and the wet/dry interface is re-evaluated. This process is repeated at every time step.

Time-varying bathymetry in ADCIRC can be enabled via changes in its existing model control parameter file and a new input file. In the model control parameter file (known as `f.15`), a new parameter can be added to request updates to the bathymetric elevations in the entire mesh (NDDT=1) or only the portion where changes occur (NDDT=2). The parameter BTIMINC specifies the time intervals at which the surface is updated, and the parameter BCHGTIMINC is the

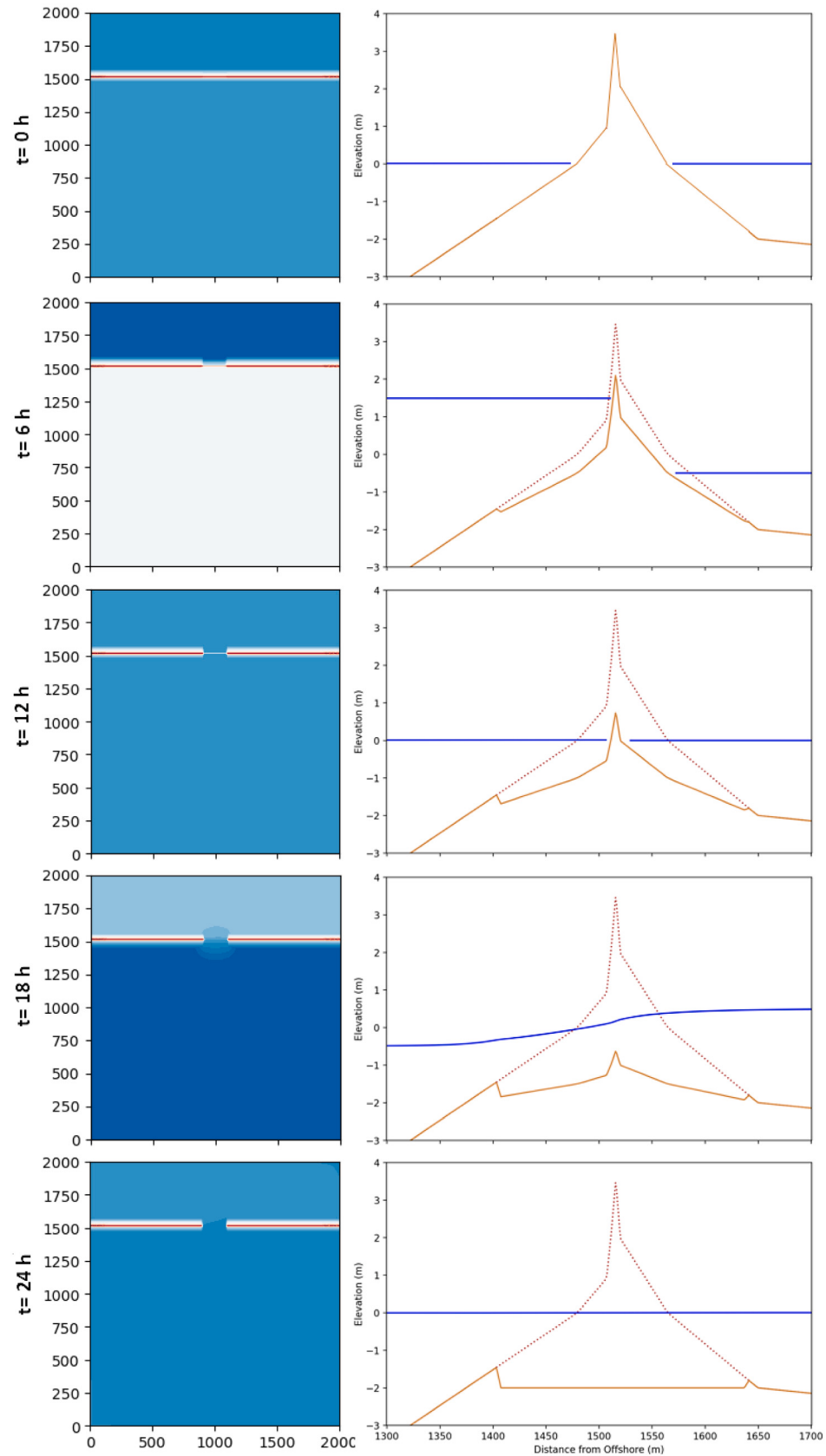


Fig. 9. Demonstration of time-varying bathymetry in ADCIRC. A breach is opened in an idealized barrier island, as shown in (left) spatial (x, y) plots and (right) cross-section (x, z) profiles. The water levels are increased at the ocean/south boundary to a maximum of 1.5 m, while the water levels in the lagoon/north are increased to a maximum of 0.5 m. At $t = 15$ h, the ground surface is lowered enough to allow flow through the breach.

duration over which the linear bathymetric changes are implemented. Time-varying data must be provided in a new input file (`fort.141`) with vertex numbers and their new bathymetric elevations. For each time interval, ADCIRC reads and updates linearly the bathymetric elevation of each vertex over the time specified by `BCHGTIMINC`. The `BCHGTIMINC` is used to control how quickly the changes to the ground elevations are implemented and can aid in model stability by “easing in” the changes rather than sudden jumps in values. Furthermore, if `BTIMINC` is a long time period, `BCHGTIMINC` can be used to more quickly implement the changes in the ground elevation during the simulation.

To demonstrate this module, a simple model of a beach with a uniform alongshore bathymetry was created. This configuration is used to resemble the breaching of a barrier island. The domain covers 2 km × 2 km of the beach, and the minimum and maximum mesh resolution are 5 m and 30 m, respectively. The bed level changes take place on a 200 m section alongshore in the middle of the domain. Over a 24-hr period, the water levels on the ocean/south boundary are increased to a maximum of 1.5 m, while the water levels in the lagoon/north are increased to a maximum of 0.5 m. The parameters are set to update the bathymetry on a one-hour (`BTIMINC=3600`) cycle, with the changes to the ground elevations occurring only during the first half hour (`BCHGTIMINC=1800`) of each cycle.

Fig. 9 (left column) shows the ground surface and water levels over time and location of breaching. The model is stable and can represent the erosion of the beach by lowering the ground surface at the mesh vertices. **Fig. 9** (right column) shows the middle cross-section and the evolution of the breach. The ground surface is lowered slowly. When the water level on the ocean exceeds the dune crest elevation, then the water flows over the dune into the back-barrier region. The wetting/drying algorithm works properly and does not introduce any instabilities to the model. We ran a set of tests to explore the sensitivity of the parameters (with `BTIMINC=3600` and `BCHGTIMINC=900`, `1800`, `3600`), however, the results did not show significant differences in the water levels or flow through the island, and no instabilities or mass imbalances were added in any cases.

References

- Beven, J.L., Cobb, H., 2003. Tropical Cyclone Report, Hurricane Isabel, 6 - 19 September 2003. Technical Report, National Hurricane Center.
- Birchler, J.J., Doran, K.S., Long, J.W., Stockdon, H.F., 2019. Hurricane Matthew: Predictions, Observations, and an Analysis of Coastal Change. Technical Report 2019-1095, U. S. Geological Survey, p. 37. <https://doi.org/10.3133/ofr20191095>.
- Blanton, B.O., Luettich, R.A., 2008. North Carolina Coastal Flood Analysis System: Model Grid Generation. Technical Report TR-08-05, Renaissance Computing Institute.
- Blanton, B.O., Madry, S., Gallupi, K., Gamiel, K., Lander, H., Reed, M., Stillwell, L., Blanchard-Montgomery, M., Luettich, R., Mattocks, C., Fulcher, C., Vickery, P., Hanson, J., Devaliere, E., McCormick, J., 2008. Report for State of North Carolina Floodplain Mapping Project Coastal Flood Analysis System. Technical Report TR-08-08, Renaissance Computing Institute.
- Bonisteel, J.M., Nayegandhi, A., Wright, C.W., Brock, J.C., Nagle, D.B., 2009. Experimental Advanced Airborne Research Lidar (EAARL) Data Processing Manual. Technical Report 2009-1078, US Geological Survey, p. 38p.
- Boujia, N., Ris, R.C., Holthuijsen, L.H., 1999. A third-generation wave model for coastal regions, Part I, Model description and validation. *J. Geophys. Res.* 104, 7649–7666. <https://doi.org/10.1029/98JC02622>.
- Canizares, R., Irish, J.L., 2008. Simulation of storm-induced barrier island morphodynamics and flooding. *Coast. Eng.* 55, 1089–1101. <https://doi.org/10.1016/j.coastaleng.2008.04.006>.
- Clinch, A.S., Russ, E.R., Oliver, R.C., Mitasova, H., Overton, M.F., 2012. Hurricane Irene and the Pea Island Breach: Pre-storm characterization and storm surge estimation using geospatial technologies. *Shore & Beach* 80, 1–10.
- Cox, A.T., Greenwood, J.A., Cardone, V.J., Swail, V.R., 1995. An interactive objective kinematic analysis system. In: Dawson, C.N., Gerritsen, M. (Eds.), Proceedings of the Fourth International Workshop on Wave Hindcasting and Forecasting, pp. 109–118.
- Cyriac, R., Dietrich, J.C., Fleming, J.G., Blanton, B.O., Kaiser, C., Dawson, C.N., Luettich, R.A., 2018. Variability in coastal flooding predictions due to forecast errors during Hurricane Arthur (2014). *Coast. Eng.* 137, 59–78. <https://doi.org/10.1016/j.coastaleng.2018.02.008>.
- de Vet, P., 2014. Modelling Sediment Transport and Morphology During Overwash and Breaching Events (Master's thesis). Delft University of Technology, Delft, ND.
- Dietrich, J.C., Bunya, S., Westerink, J.J., Ebersole, B.A., Smith, J.M., Atkinson, J.H., Jensen, R.E., Resio, D.T., Luettich, R.A., Dawson, C.N., Cardone, V.J., Cox, A.T., Powell, M.D., Westerink, H.J., Roberts, H.J., 2010. A high-resolution coupled riverine flow, tide, wind, wind wave and storm surge model for southern Louisiana and Mississippi: Part II – synoptic description and analysis of Hurricanes Katrina and Rita. *Mon. Weather Rev.* 138, 378–404. <https://doi.org/10.1175/2009MWR2907.1>.
- Dietrich, J.C., Dawson, C.N., Proff, J., Howard, M.T., Wells, G., Fleming, J.G., Luettich, R.A., Westerink, J.J., Cobell, Z., Vitse, M., 2013. Real-time forecasting and visualization of hurricane waves and storm surge using SWAN+ADCIRC and FigureGen. In: Dawson, C.N., Gerritsen, M. (Eds.), Computational Challenges in the Geosciences. pp. 49–70. https://doi.org/10.1007/978-1-4614-7434-0_3.
- Dietrich, J.C., Muhammad, A., Curcic, M., Fathi, A., Dawson, C.N., Chen, S.S., Luettich, R.A., 2018. Sensitivity of storm surge predictions to atmospheric forcing during Hurricane Isaac. *J. Waterway Port Coast. Ocean Eng.* 144, [https://doi.org/10.1061/\(ASCE\)WW.1943-5460.0000419](https://doi.org/10.1061/(ASCE)WW.1943-5460.0000419).
- Dietrich, J.C., Trahan, C.J., Howard, M.T., Fleming, J.G., Weaver, R.J., Tanaka, S., Yu, L., Luettich, R.A., Dawson, C.N., Westerink, J.J., Wells, G., Lu, A., Vega, K., Kubach, A., Dresback, K.M., Kolar, R.L., Kaiser, C., Twilley, R.R., 2012. Surface trajectories of oil transport along the Northern Coastline of the Gulf of Mexico. *Cont. Shelf Res.* 41, 17–47. <https://doi.org/10.1016/j.csr.2012.03.015>.
- Dietrich, J.C., Westerink, J.J., Kennedy, A.B., Smith, J.M., Jensen, R.E., Zijlema, M., Holthuijsen, L.H., Dawson, C.N., Luettich, R.A., Powell, M.D., Cardone, V.J., Cox, A.T., Stone, G.W., Pourtaheri, H., Hope, M.E., Tanaka, S., Westerink, L.G., Westerink, H.J., Cobell, Z., 2011a. Hurricane Gustav (2008) waves and storm surge: Hindcast, validation and synoptic analysis in Southern Louisiana. *Mon. Weather Rev.* 139, 2488–2522. <https://doi.org/10.1175/2011MWR3611.1>.
- Dietrich, J.C., Zijlema, M., Westerink, J.J., Holthuijsen, L.H., Dawson, C.N., Luettich, R.A., Jensen, R.E., Smith, J.M., Stelling, G.S., Stone, G.W., 2011b. Modeling hurricane waves and storm surge using integrally-coupled, scalable computations. *Coast. Eng.* 58, 45–65. <https://doi.org/10.1016/j.coastaleng.2010.08.001>.
- Elsayed, S.M., Oumeraci, H., 2017. Effect of beach slope and grain-stabilization on coastal sediment transport: An attempt to overcome the erosion overestimation by XBeach. *Coast. Eng.* 121, 179–196. <https://doi.org/10.1016/j.coastaleng.2016.12.009>.
- Elsayed, S.M., Oumeraci, H., Goseberg, N., 2018. Erosion and breaching of coastal barriers in a changing climate: Associated processes and implication for contamination of coastal aquifers. In: Coastal Engineering Proceedings, vol. 1. p. papers.107. <https://doi.org/10.9753/icce.v36.papers.107>.
- Emanuel, K., 2020. Evidence that hurricanes are getting stronger. *Proc. Natl. Acad. Sci. USA* 117, 13194–13195. <https://doi.org/10.1073/pnas.2007742117>.
- Engelstad, A., Ruessink, B.G., Wesselman, D., Hoekstra, P., Oost, A., van der Vegt, M., 2017. Observations of waves and currents during barrier island inundation. *J. Geophys. Res. Oceans* 122, 3152–3169.
- Fearnley, S.M., Miner, M.D., Kulp, M., Bohling, C., Penland, S., 2009. Hurricane impact and recovery shoreline change analysis of the Chandeleur Islands, Louisiana, USA: 1855 to 2005. *Geo-Mar Lett.* 29, 455–466.
- FEMA, 2020. Hurricane Michael in Florida: Building Performance Observations, Recommendations, and Technical Guidance. Technical Report FEMA P-2077, Federal Emergency Management Agency.
- Fredericks, X., Kranenburg, C.J., Nagle, D.B., 2017. EAARL Coastal Topography-Cape Hatteras, North Carolina, Pre- and Post-Hurricane Isabel, 2003. <https://doi.org/10.5066/F76W9879>, US Geological Survey data release.
- Fritz, H.M., Blount, C., Sokolski, R., Singleton, J., Fuggle, A., McAdoo, B.G., Moore, A., Grass, C., Tate, B., 2007. Hurricane Katrina storm surge distribution and field observations on the mississippi barrier islands. *Estuarine, Coastal, and Shelf Science* 74, 12–20. <https://doi.org/10.1016/j.ecss.2007.03.015>.
- Gharagozlu, A., Dietrich, J.C., Karanci, A., Luettich, R.A., Overton, M.F., 2020. Storm-driven erosion and inundation of barrier islands from dune- to region-scales. *Coast. Eng.* 158 (103674), <https://doi.org/10.1016/j.coastaleng.2020.103674>.
- Gracia, V., Garcia, M., Grifoll, M., Sanchez-Arcilla, A., 2013. Breaching of a barrier under extreme events. The role of morphodynamic simulations. *J. Coast. Res.* 65, 951–956. <https://doi.org/10.2112/SI65-161.1>.
- Grzegorzewski, A.S., Cialone, M., Lansen, A.J., van Ledden, M., Smith, J., Wamsley, T., 2009. The influence of barrier islands on hurricane-generated storm surge and waves in Louisiana and Mississippi. In: Coastal Engineering 2008. pp. 1037–1049. https://doi.org/10.1142/9789814277426_0087.
- Grzegorzewski, A.S., Cialone, M.A., Wamsley, T.V., 2011. Interaction of barrier islands and storms: Implications for flood risk reduction in Louisiana and Mississippi. *J. Coast. Res.* 59, 156–164. <https://doi.org/10.2112/SI59-016.1>.
- Hope, M.E., Westerink, J.J., Kennedy, A.B., Kerr, P.C., Dietrich, J.C., Dawson, C.N., Bender, C.J., Smith, J.M., Jensen, R.E., Zijlema, M., Holthuijsen, L.H., Luettich, Jr., R.A., Powell, M.D., Cardone, V.J., Cox, A.T., Pourtaheri, H., Roberts, H.J., Atkinson, J.H., Tanaka, S., Westerink, H.J., Westerink, L.G., 2013. Hindcast and validation of Hurricane Ike (2008) waves, forerunner, and storm surge. *J. Geophys. Res. Oceans* 118, 4424–4460. <https://doi.org/10.1002/jgrc.20314>.
- Hovis, J., Popovich, W., Zervas, C., Hubbard, J., Shih, H.H., Stone, P., 2004. Effects of hurricane isabel on water levels data report, April 2004. Technical Report, National Oceanic and Atmospheric Administration.

- Kossin, J.P., Knapp, K.P., Olander, T.L., Velden, C.S., 2020. Global increase in major tropical cyclone exceedance probability over the past four decades. *Proc. Natl. Acad. Sci. USA* 117, 11975–11980. <https://doi.org/10.1073/pnas.1920849117>.
- Kurum, M.O., Overton, M.F., 2013. Scenario testing on the impact of topography, land cover and sea-level rise on barrier island breaching, in: *Proceedings of Coastal Dynamics 2013*, pp. 1025–1036.
- Luettich, R.A., Westerink, J.J., Scheffner, N.W., 1992. ADCIRC: An Advanced Three-Dimensional circulation model for shelves coasts and estuaries, report 1: Theory and methodology of ADCIRC-2DDI and ADCIRC- 3DL. Technical Report, United States Army Corps of Engineers.
- McCall, R.T., van Thiel de Vries, J.S.M., Plant, N.G., van Dongeren, A.R., Roelvink, J.A., Thompson, D.M., Reniers, A.J.H.M., 2010. Two-dimensional time dependent hurricane overwash and erosion modeling at santa rosa island. *Coast. Eng.* 57, 668–683. <https://doi.org/10.1016/j.coastaleng.2010.02.006>.
- Miselis, J.L., Andrews, B.D., Nicholson, R.S., Defne, Z., Ganju, N.K., Navoy, A., 2016. Evolution of mid-Atlantic Coastal and back-BARRIER Estuary environments in response to a hurricane: Implications for barrier-estuary connectivity. *Estuar. Coasts* 39, 916–934. <https://doi.org/10.1007/s12237-015-0057-x>.
- Mitasova, H., Mitas, L., Harmon, R.S., 2005. Simultaneous spline approximation and topographic analysis for lidar elevation data in open-source GIS. *IEEE Geosci. Remote Sens. Lett.* 2, 375–379.
- Morton, R.A., 2002. Factors controlling storm impacts on coastal barriers and beaches – a preliminary basis for near real-time forecasting. *J. Coast. Res.* 18 (3), 486–501, URL <http://www.jstor.org/stable/4299096>.
- Mulligan, R.P., Walsh, J.P., Wadman, H.M., 2015. Storm surge and surface waves in a shallow lagoonal estuary during the crossing of a hurricane. *J. Waterw. Port Coast. Ocean Eng.* 141, [https://doi.org/10.1061/\(ASCE\)WW.1943-5460.0000260](https://doi.org/10.1061/(ASCE)WW.1943-5460.0000260).
- Nederhoff, G.M., 2014. Modeling the Effects of Hard Structures on Dune Erosion and Overwash: Hindcasting the Impact of Hurricane Sandy on New Jersey with XBeach (Master's thesis). Delft University of Technology, Delft, ND.
- Passeri, D.L., Hagen, S., Bilskie, M., Medeiros, S.C., 2015. On the significance of incorporating shoreline changes for evaluating coastal hydrodynamics under sea level rise scenarios. *Nat. Hazards* 75 (2), 1599–1617. <https://doi.org/10.1007/s11069-014-1386-y>.
- Passeri, D.L., Long, J.W., Plant, N.G., Bilskie, M.V., Hagen, S.C., 2018. The influence of bed friction variability due to land cover on storm-driven barrier island morphodynamics. *Coast. Eng.* 132, 82–94. <https://doi.org/10.1016/j.coastaleng.2017.11.005>.
- Pierce, J.W., 1970. Tidal inlets and washover fans. *J. Geology* 78, 230–234.
- Rego, J.L., Li, C., 2010. Storm surge propagation in Galveston Bay during Hurricane Ike. *J. Mar. Syst.* 82 (4), 265–279. <https://doi.org/10.1016/j.jmarsys.2010.06.001>.
- Riggs, S.R., Cleary, W.J., Snyder, S.W., 1995. Influence of inherited geologic framework on barrier shoreface morphology and dynamics. *Mar. Geol.* 126, 213–234. [https://doi.org/10.1016/0025-3227\(95\)00079-E](https://doi.org/10.1016/0025-3227(95)00079-E).
- Roelvink, J.A., 1993. Dissipation in random wave groups incident on a beach. *Coast. Eng.* 19, 127–150. [https://doi.org/10.1016/0378-3839\(93\)90021-Y](https://doi.org/10.1016/0378-3839(93)90021-Y).
- Roelvink, D., Reniers, A.J.H.M., van Dongeren, A., van Thiel de Vries, J., McCall, R., Lescinski, J., 2009. Modelling storm impacts on beaches, dunes and barrier islands. *Coast. Eng.* 56, 1133–1152. <https://doi.org/10.1016/j.coastaleng.2009.08.006>.
- Rogers, S.M., Tezak, E.S., 2004. Hurricane Isabel damage to coastal North Carolina buildings. *Shore & Beach* 72 (2), 38–44.
- Safak, I., Warner, J.C., List, J.H., 2016. Barrier island breach evolution: Alongshore transport and bay-ocean pressure gradient interactions. *J. Geophys. Res. Oceans* 121, 8720–8730. <https://doi.org/10.1002/2016JC012029>.
- Sallenger, A.H., 2000. Storm impact scale for barrier islands. *J. Coast. Res.* 16, 890–895.
- Sallenger, A.H., Wright, C.W., Guy, K., Morgan, K., 2004. Assessing storm-induced damage and dune erosion using Airborne Lidar: Examples from Hurricane Isabel. *Shore & Beach* 72, 25–29.
- Sallenger, A.H., Wright, C.W., Lillycrop, J., Howd, P., Stockdon, H., Guy, K.K., Morgan, K., 2007. Extreme changes to barrier islands along the central Gulf of Mexico coast during Hurricane Katrina. In: Farris, G.S., Smith, G.J., Crane, M.P., Demas, C.R., Robbins, L.L., Lavoie, D.L. (Eds.), *Science and the Storms: The USGS Response To the Hurricanes of 2005*, vol. 1306. United States Geological Survey, pp. 113–118.
- Schambach, L., Grilli, A.R., Grilli, S.T., Hashemi, M.R., King, J.W., 2018. Assessing the impact of extreme storms on barrier beaches along the Atlantic coastline: Application to the southern Rhode Island coast. *Coast. Eng.* 133, 26–42. <https://doi.org/10.1016/j.coastaleng.2017.12.004>.
- Sebastian, A.G., Proft, J.M., Dietrich, J.C., Du, W., Bedient, P.B., Dawson, C.N., 2014. Characterizing hurricane storm surge behavior in Galveston bay using the SWAN+ADCIRC model. *Coast. Eng.* 88, 171–181. <https://doi.org/10.1016/j.coastaleng.2014.03.002>.
- Sheng, Y.P., Alymov, V., Paramygin, V.A., 2010. Simulation of storm surge, wave, currents, and inundation in the Outer Banks and Chesapeake Bay during Hurricane Isabel in 2003: The importance of waves. *J. Geophys. Res.* 115, C04008. <https://doi.org/10.1029/2009JC005402>.
- Sherwood, C.R., Brown, J., Kranenburg, C., Ritchie, A., Warrick, J., Wright, W., Aretxabaleta, A., Zeigler, S., Thompson, D.M., Plant, N.G., 2020. Morphologic Changes from Sound-Side Inundation of North Core Banks, Cape Lookout National Seashore, North Carolina, USA during Hurricane Dorian. U. S. Geological Survey, URL <https://osm2020.agu.ipostersessions.com/default.aspx?s=3C-50-D3-39-85-4F-24-F1-96-82-D6-5E-80-28-21-CA>.
- Sherwood, C.R., Long, J.W., Dickhudt, P.J., Dalyander, P.S., Thompson, D.M., Plant, N.G., 2014. Inundation of a barrier island (Chandeleur Islands, Louisiana, USA) during a hurricane: Observed water-level gradients and modeled seaward sand transport. *J. Geophys. Res. Earth Surf.* 119, 1498–1515. <https://doi.org/10.1002/2013JF003069>.
- Smalley, S.M., Irish, J.L., 2017. Barrier island morphological change by bay-side storm surge. *J. Waterw. Port Coast. Ocean Eng.* 143, 04017025. [https://doi.org/10.1061/\(ASCE\)WW.1943-5460.0000413](https://doi.org/10.1061/(ASCE)WW.1943-5460.0000413).
- Sopkin, K.L., Stockdon, H.F., Doran, K.S., Plant, N.G., Morgan, K.L.M., Guy, K.K., Smith, K.E.L., 2014. Hurricane Sandy: Observations and analysis of coastal change. (2014–1088), U. S. Geological Survey, p. 54. <https://doi.org/10.3133/ofr20141088>.
- Suh, S.W., Lee, H.Y., Kim, H.J., Fleming, J.G., 2015. An efficient early warning system for typhoon storm surge based on time-varying advisories by coupled ADCIRC and SWAN. *Ocean Dyn.* 65, 617–646. <https://doi.org/10.1007/s10236-015-0820-3>.
- Svendsen, A., 1984. Wave heights and set-up in a surf-zone. *Coast. Eng.* 8, 303–329. [https://doi.org/10.1016/0378-3839\(84\)90028-0](https://doi.org/10.1016/0378-3839(84)90028-0).
- Thomas, A., Dietrich, J.C., Asher, T.G., Blanton, B.O., Cox, A.T., Dawson, C.N., Fleming, J.G., Luettich, R.A., 2019. Influence of storm timing and forward speed on tide-surge interactions during Hurricane Matthew. *Ocean Model.* 137, 1–19. <https://doi.org/10.1016/j.ocemod.2019.03.004>.
- Thornton, E.B., MacMahan, J., Sallenger, A.H., 2007. Rip currents, mega-cusps, and eroding dunes. *Mar. Geol.* 240, 151–167. <https://doi.org/10.1016/j.margeo.2007.02.018>.
- van der Lugt, M.A., Quataert, E., van Dongeren, A., van Ormondt, M., 2019. Morphodynamic modeling of the response of two barrier islands to atlantic hurricane forcing. *Estuar. Coast. Shelf Sci.* 229 (106404), <https://doi.org/10.1016/j.ecss.2019.106404>.
- van Ormondt, M., Nelson, T.R., Hapke, C.J., Roelvink, J.A., 2020. Morphodynamic modelling of the wilderness breach, Fire Island, New York. Part I: Model set-up and validation. *Coast. Eng.* 157 (103621), <https://doi.org/10.1016/j.coastaleng.2019.103621>.
- Velasquez, L., Sciaudone, E.J., Mitasova, H., Overton, M.F., 2015. Multi-temporal geospatial analysis of the evolution and closing of Pea Island Breach, NC. In: *Proceedings of Coastal Sediments 2015*. World Scientific, pp. 1–11.
- Wamsley, T.V., Cialone, M.A., Smith, J.M., Ebersole, B.A., Grzegorzevski, A.S., 2009. Influence of landscape restoration and degradation on storm surge and waves in Southern Louisiana. *J. Natural Hazards* 51, 207–224. <https://doi.org/10.1007/s11069-009-9378-z>.
- Wamsley, T.V., Hathaway, K.K., 2004. Monitoring morphology and currents at the Hatteras breach. *Shore & Beach* 72, 9–14.
- Westerink, J.J., Luettich, Jr., R.A., Feyen, J.C., Atkinson, J.H., Dawson, C.N., Roberts, H.J., Powell, M.D., Dunion, J.P., Kubatko, E.J., Pourtaheri, H., 2008. A basin to channel scale unstructured grid hurricane storm surge model applied to Southern Louisiana. *Mon. Weather Rev.* 136, 833–864. <https://doi.org/10.1175/2007MWR1946.1>.
- Wurtkowski, M., 2004. Hatteras breach closure. *Shore & Beach* 72, 20–24.
- Zijlema, M., 2010. Computation of wind-wave spectra in coastal waters with SWAN on unstructured grids. *Coast. Eng.* 57, 267–277. <https://doi.org/10.1016/j.coastaleng.2009.10.011>.